AIMS Energy, 10(4): 922–942.
DOI: 10.3934/energy.2022042
Received: 18 May 2022
Revised: 29 July 2022
Accepted: 31 July 2022
Published: 04 August 2022

http://www.aimspress.com/journal/energy

Review

Novel designs of thermoelectric generator for automotive waste heat recovery: A review

Tan Nguyen Tien[1,2], Quang Khong Vu[1,*], Vinh Nguyen Duy[3,*]

[1] Department of Vehicle and Energy Conversion Engineering, School of mechanical engineering, Hanoi University of Science and Technology, Vietnam
[2] Department of Student Affairs, Hanoi University of Industry, Vietnam
[3] Faculty of Vehicle and Energy Engineering, Phenikaa University, Vietnam

* **Correspondence:** Email: vinh.nguyenduy@phenikaa-uni.edu.vn, Quang.khongvu@hust.edu.vn; Tel: +84985814118.

Abstract: Many worldwide scientists have concentrated on using waste heat recovery technology in automotive applications because of increasingly strict fuel consumption. The thermoelectric generator (TEG) has garnered significant interest in the automobile sector as a viable waste heat recovery solution over the past several decades. A short survey of thermoelectric materials and heat exchangers for TEG systems is initially presented in this paper. To overcome the heat exchanger's current shortcomings, some previous studies designed a variety of the heat exchanger geometry of the TEG system. They suggested concentric cylindrical TEG system utilizes an annular thermoelectric module instead of the traditional square-shaped one. It uses the heat pipe's benefits to improve radial heat transmission. A comparison of the water-inside and gas-inside arrangements indicated that the water-inside concentric cylindrical TEG system provided a greater power output in our simulations to test the performance of the proposed system.

Keywords: automotive waste heat recovery; thermoelectric generator; thermoelectric cooler; Seebeck effect, Peltier effect

1. Introduction

For several decades, environmental degradation and global warming have resulted from fossil

fuels like gasoline and diesel fuel in energy generation. Continued reliance on fossil fuels will soon hit a tipping point regarding sustainability. As a result, using carbon-free renewable energy derived from geothermal, solar, and other natural sources and converting it to valuable energy has garnered significant interest. Thermal energy is plentiful and comes from various sources, including electrical devices, buildings, air conditioners, and especially internal combustion engines (ICEs).

The use of a thermoelectric generator (TEG) is one of the best solutions to improve the overall efficiency of ICEs [1–6]. A TEG is a device that converts heat into electricity. TEGs are promising for attaining a low-carbon society since they can produce electrical energy from waste heat. However, current TEG systems' relatively poor conversion efficiency has hindered the widespread use of TEGs for power production. The conversion efficiency of TEGs must be enhanced to be more extensively accepted.

TEGs will be the focus of this article, which aims to provide a complete overview of the field. In contrast to prior work, this work presents the many kinds (planar, vertical, and mixed) and technologies (silicon, ceramics, and polymers) of TEGs. Using a variety of thermoelectric material arrangements, we want to research the most recent thermoelectric materials and keys to provide high power factor efficiency (conventional, segmented, and cascaded).

2. Thermoelectric fundamentals

With thermoelectrics, waste heat and cooling applications may be harnessed in an environmentally friendly manner. Navigating the interaction between electrical and heat transfer is critical to designing high-performance thermoelectrics [7]. This requires an in-depth knowledge of electron and phonon scattering physics, as well as the optimization of entropy and electronic transport symmetry breaking. Thermoelectric effects are reversible processes that directly convert heat energy to electrical energy. Direct energy conversion is based on the thermoelectric materials' physical transport qualities (thermal conductivity, electric conductivity, and Seebeck coefficient) and their energy conversion efficiency (figure-of-merit). The Seebeck effect is employed in thermoelectric generators, often used to convert heat energy to electrical energy. Charge carriers travel from the hot to the cold side of a conductive substance when a temperature gradient is introduced. Charge buildup causes an electric potential difference in the case of an open circuit. TEGs have several benefits, including design simplicity, the lack of moving parts, a long lifespan, minor maintenance, and environmental friendliness (no chemical compounds). To boost the output power, TEGs are frequently constructed up of numerous coupled thermopiles [8–10]. Each thermopile comprises a few thermocouples (TCs) electrically linked in series and thermally associated in parallel. The thermocouple consists of two materials with opposing Seebeck coefficients connected at their ends. Due to the Seebeck effect, the appearance of a temperature gradient between the two TCs ends generates an electric voltage defined by Eq (1):

$$V_{out} = N\alpha\Delta_T \tag{1}$$

where N is the number of connected thermocouples, α is the Seebeck coefficients of the two joined materials forming the thermocouple, and Δ_T is the temperature gradient.

For the most part, the Seebeck effect or heat transfer may be accomplished using a single Peltier element (via the Peltier effect). One Peltier element can only provide so much power before it becomes ineffective. Many n- and p-type semiconductor Peltier components are used in commercial Peltier

devices to maximize output power. The individual components are linked together in a sequence using metallic connectors. Due to the absence of a barrier potential at the junctions between the semiconductors, charge carriers may flow freely in both directions. The n-type and the p-type heat flow in the same direction via the different Peltier device components. All the Peltier device's pieces consist of two ceramic plates sandwiched between a series of p-n pairs linked with copper. This design maximizes the available surface area for heat pump cooling and heating applications. Having a larger surface area also helps to absorb and generate electricity from waste heat (through the Seebeck effect).

3. Designs of thermoelectric generators for automotive waste heat recovery

3.1. Energy balance of internal combustion engines

The thermal efficiency of vehicle internal combustion engines typically varies between 15% and 40%, depending on operating circumstances and engine design. The remaining 60–85% of fuel energy is lost to the environment as waste heat, mainly via the radiator and exhaust system. Depending on the operating circumstances of the engine, between 30% and 50% of total fuel energy may be emitted via the radiator, with larger values happening at lower engine loads [11–15]. To comprehend the fundamental causes of energy dissipation, an essential energy balance for an ICE may be established, considering in-cylinder operations under steady-state operating circumstances. A simplified energy balance may be expressed as follows regarding the simplified diagram depicted in Figure 1.

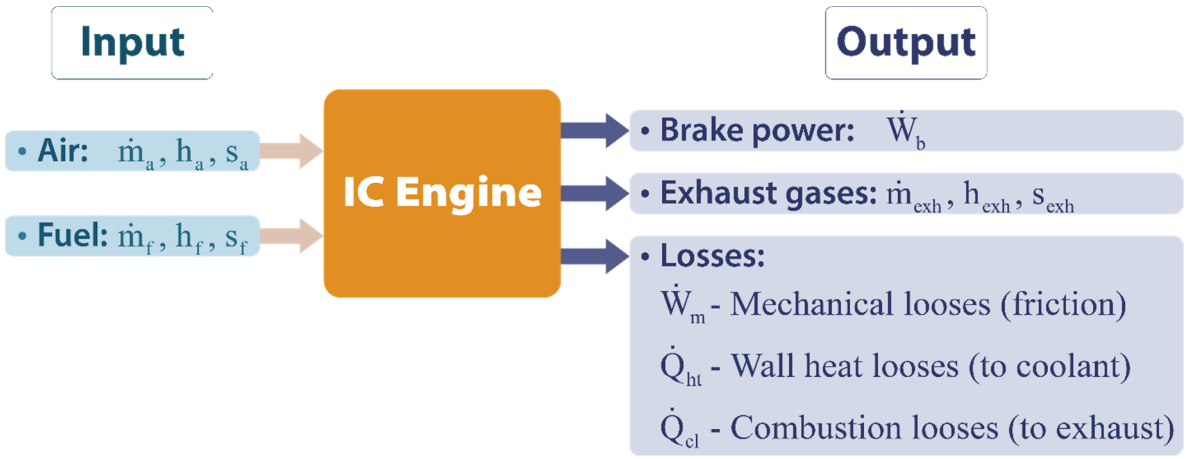

Figure 1. Control volume of IC engine showing energy flows.

$$\left(\dot{m}_f Q_{LHV} + \dot{Q}_{ht} + \dot{Q}_{cl}\right) - \left(\dot{W}_b + \dot{W}_m\right) = \dot{m}_{exh} h_{exh} - \left(\dot{m}_a h_a + \dot{m}_f h_f\right) \quad (2)$$

where Q_{LHV} is the lower heating value of the fuel (kJ/kg), $\dot{Q}_{ht}$ is the heat transfer losses through the wall, $\dot{Q}_{cl}$ is the incomplete combustion product losses, $\dot{W}_b$ is the brake power, $\dot{W}_m$ is the friction losses, $\dot{m}$ is the mass flow rate, and h is the sensible enthalpy associated with the air, fuel, and exhaust gases. The three key energy balancing terms are braking power, cooling heat loss, and exhaust heat loss [16–20]. Unaccounted energy losses are often referred to as miscellaneous energy losses. The significant contributions to this topic demonstrate that thermal energy rejected to the coolant and

exhaust gases is the primary cause of energy and availability losses in internal combustion engines. This lays the groundwork for the development of engine design and system integration solutions to reduce engine energy dissipation. For the TEG application, lower temperatures reduce absorber efficiency because of increased TEG viscosity, but higher temperatures cause greater TEG vaporization losses. The ideal feed gas temperature range for the absorber is generally 299.8 K–310.9 K. Mid-range flash drum pressure 430.8 kPa is used, and the lean TEG temperature is adjusted 15 F higher than the gas temperature exiting the contactor, resulting in a 15-degree temperature difference. Thus, the heat loss due to the exhaust gas and cooling water is suitable for the operation of the heat utilization system using TEG.

3.2. Thermoelectric materials for TEG fabrication

The maximum efficiency of a thermoelectric material for thermoelectric power generation and cooling is determined by the dimensionless figure of merit ZT, which is defined as:

$$ZT = \frac{S^2\sigma}{k}T \tag{3}$$

where S denotes the Seebeck coefficient, ρ denotes the electrical resistivity, k denotes the thermal conductivity, and T is the material's absolute temperature. For the most part, the figure of merit (ZT) is a temperature-dependent material parameter determined from the temperature-dependent material properties. For these material qualities to vary from one end of the thermoelectric generator to another, an effective thermoelectric generator must operate across a restricted temperature difference ΔT. In most thermoelectric material research, the primary emphasis is the scientific ideas that underpin their thermal characteristics.

Many thermoelectric materials are being explored for power generation applications, such as GeTe [21], PbTe [22], half Heuslers [23], Bi_2Te_3 [24] and silicides [25]. Nanostructuring these materials into a layered superlattice structure with alternating Bi_2Te_3 and Sb_2Te_3 layers results in a device with solid electrical conductivity but poor heat conductivity perpendicular to it. At room temperature, bismuth telluride and its solid solutions are excellent thermoelectric materials, making them useful for refrigeration applications below 300 K. Single crystalline bismuth telluride compounds have been grown using the Czochralski process. Directional solidification from melt or powder metallurgical methods is often used to make these compounds. Due to crystal grains' random orientation, these materials are less efficient than single-crystalline materials. Still, their mechanical characteristics are greater, and their susceptibility to structural faults and impurities is reduced due to the high optimum carrier concentration.

As mentioned in many previous studies, Bismuth telluride alloys, lead telluride alloys, silicon-germanium alloys, antimony telluride, and tin selenide are all examples of conventional TE materials. This inorganic thermoelectrics was developed during the 50 s and 60 s of the last centuries. The greatest ZT value of the developed inorganic TE materials remained nearly equal until the mid-1990s, which was not cost-effective in most applications [21]. However, developments in science and technology, as well as increased awareness of the dangers of fossil fuels, resulted in a strong desire to enhance the performance (as measured by ZT) of TE materials. As a result, since the mid-1990s, TE research has mainly concentrated on improving the TE characteristics of inorganic TE materials by increasing their Seebeck coefficient and thermal conductivity. Sb_2Te_3, Bi_2Te_3, Bi_2Se_3, PbTe, SnTe, and SnS and related

alloys have been the most promising inorganic TE materials for room temperature (300–400 K) operation since the 1950s [26,27]. The next generation of TE materials will be higher multinary bulk materials, the majority of which will be discovered using sophisticated material screening techniques. High-throughput computational material screening, a fundamental component of the Materials Genome Initiative, is one possible way [30,31]. Gibbs et al. proposed a "Femi Surface Complexity Factor" as an indication for high-performance TE materials, based on the number of pockets and anisotropy of the Fermi surface [32]. The configurational entropy of material was suggested by Liu et al. as a relevant indicator [33]. The TE study of PbSnTeSe, (BiSbTe1.5Se1.5)1-xAgx, and AlxCoCrFeNi are in line with high entropy thermoelectrics. A website by Gaultois et al., which uses the Herfindahl-Hirschman index as a merit measure, gives relevant information on numerous potential materials [34]. Even with a long stride, calculating the whole set of TE characteristics of a particular material from fundamental principles remains difficult [35]. Some existing strategies to boost thermoelectric material performance have also been mentioned in [36–38].

3.3. Application of TEG for heat recovery from the vehicle

The exhaust pipe and radiator of automobiles powered by internal combustion engines may be repurposed using thermoelectric technology. Various TEGs are installed around the car to produce power from the vehicle's waste heat. When waste energy from the car is appropriately used, diesel fuel consumption is minimized since the generator used for battery charging and other low energy demands in the vehicle are eliminated [39,40]. The exhaust pipe is the best place to harvest waste heat from a vehicle since it is the most likely location to find high temperatures. Therefore, it should be mentioned that if TE technology progresses, it will be feasible to reduce fuel consumption by 10% in the near future.

Some studies have looked at how waste heat may be converted into useable electric power utilizing TE. A prototype car was used to evaluate the TEG's performance characteristics, and an energy harvesting system based on TEG was built to gather electricity from the vehicle's exhaust pipe [40]. The system's features include cold and hot side temperatures, power output, open circuit voltage (OCV), and maximum power. As a result of the TEG system, road, and rotating drum tests, the highest outputs were 183.24 W, 600 W, and 944 W, with efficiency percentages of 0.9 percent, 1.28 percent, and 1.85%, respectively. An independent cooling system isn't straightforward; thus, an experimental vehicle is kept immobile while being cooled by an oscillating spinning drum test table with a fan system. A large quantity of energy may be recovered from waste heat using the manufactured TEG gadget. However, the fundamental difficulty is improving the exhaust pipe to reduce thermal contact and enhance hot side temperature, which will lead to increased produced power from TE. Fourier's law and the Seebeck effect are used to analyze the TEG implanted in the exhaust pipe of cars [41]. Adjusting the convection heat transfer coefficient of the high-temperature side instead of the low-temperature-sid significantly increases the TEG power output and efficiency. The power and efficiency of the TEG are maximized during impedance matching when internal resistance is the same as external resistance. Moreover, when ZT is raised, the maximum value shifts toward a rising ratio of external resistance to internal resistance. Although the ratio of external resistance to internal resistance increases due to an increase in ZT, the maximum TEG power is also increasing. A fresh suggestion is proposed to increase the TEG's performance with the new experimental design in mind. TEG's power output and efficiency may be increased by using the appropriate phase change material, which is made possible by using

phase change materials to boost the heat transfer property of the high-temperature side. To evaluate the TEG module's performance, test benches are also built for energy harvesting [42]. A maximum power output of 183.24 W at 3200 r/mi engine rotation was determined by examining the engine's maximum power output and testing results. Cold-side temperature, flow rate, and applied pressure have a considerable impact on the maximum power output. Bi2Te3-based thermoelectric modules may also be able to harvest low-grade exhaust thermal energy from automobile exhaust pipes, according to recent studies. New physical mechanisms have been discovered as a result of advances in materials production processes and processing technology, making high-performance thermoelectric materials even more readily available. An increasing number of in-depth reviews on a wide range of thermoelectric topics, with a special emphasis on solid-state thermoelectric processes, have been published in recent years. Even though thermoelectric materials have been obtained through bottom-up procedures, thorough studies detailing these technologies are still uncommon [43–46].

Six-stroke engines, turbocharging, turbo-compounding, exhaust gas recirculation (EGR), and waste heat recovery (WHR) were mentioned in [47]. However, the average efficiency of internal combustion engines may be as low as 15% as mentioned in many previous studies. Liming et al. claim a maximum heat recovery efficiency of 20% from an ORC [48], whereas Wei et al. record a 16% ORC efficiency in a Heavy-Duty Vehicle (HDV) [49]. The quantity of recovered power is affected by engine load, pressure, temperature, and working fluid type. The output power of an ORC from a simulation on a 2006 MY Cummins ISM 10.8 L diesel engine ranged between 1 and 9 kW [50]. The ORC, on the other hand, is a sophisticated system that needs a significant amount of steam and works with high-temperature and pressure steam, as well as moving components. Furthermore, since an ORC has a considerable time constant, the system's power requirement may be low when the quantity of recovered power is significant. This problem generates a mismatch between demand and electricity production, which is challenging to manage. Another issue for the ORC is the vast number of components, which results in a very significant mass. As a result, the ORC is a less appealing alternative for automotive applications. Still, it may be more appropriate for maritime or stationary power generators where power consumption is relatively steady over time and space and weight are not as crucial as in a car.

3.4. Heat exchanger profile designs

Heat exchangers (HEXs) are devices that efficiently transfer heat from one medium to another. The following is a brief overview of HEXs and related technologies for enhancing heat transfer. HEXs may be categorized in a variety of ways. For example, HEXs may be classified as parallel flow, counterflow, or crossflow according to how they flow. The contact mechanism between hot and cold fluids is recuperative, regenerative, and direct contact. Heat exchangers may also be divided into several types based on their mechanism, such as double pipe, shell and tube, spiral tube, gasket, spiral plate, lamella, finned plate, and lastly, finned tube. Heat exchanger selection is a significant difficulty since many different kinds of HEXs. The constraints of each heat exchanger type should be considered before selecting the best design. It is essential to consider manufacturing costs and a variety of other factors such as temperature ranges and pressure restrictions and the effects of these factors on thermal performance and pressure drop, and the flow capacity of various fluids.

3.4.1. Heat changer thermodynamics

Regardless of form or design, heat exchangers work under the Zeroth, First and Second Laws of Thermodynamics, which govern the transfer or exchange of heat between two fluids [51–55]. And thus, Understanding the three methods of heat transmission, including conduction, convection, and radiation, supports a better comprehend heat exchanger thermodynamics [56–60].

The movement of a fluid, such as air or water, causes heat to be transferred from a heated surface through convection [61–65]. When heated, most liquids expand, becoming less dense and rising in the fluid's colder regions. Another way, when a room is heated, the hot air rises to the roof because it is less dense and therefore more easily transferred heat energy, colliding with colder air and returning to the ground as it cools. Free or natural convection currents are formed as a result of this procedure. When sing a hydronic heating system, heated water is pushed through a pipe, resulting in convection via a process known as forced or aided convection.

Meanwhile, the transfer of heat energy from one substance to another via direct physical contact is called conduction [66,67]. Warmer objects (those with a more significant temperature) have more molecular motion, measured by temperature as an average of the kinetic energy of molecules in the material. There is a thermal energy transfer when a hot item comes into contact with a cold object (lower in temperature). The cooler object becomes more energetic, while the hotter object becomes less electrified. There is no end to this process until thermal equilibrium has been attained. The emission of electromagnetic waves by a heated surface or item is known as thermal radiation, and it is a method of transferring heat energy. There is no need for an intermediary medium to transport the wave energy for thermal radiation. Thermal radiation is emitted by all things that are above absolute zero in a typical wide spectral range. The Stefan-Boltzmann Law may represent the net rate of radiation heat loss.

Some prior studies in the literature have been conducted under an isothermal heat source setting, where the hot side is maintained at a constant temperature. A constant heat source (isoflux) such as radiating furnace walls or convective exhaust gas is possible in practical applications. There is some overlap between the isothermal and isoflux heat source scenarios. A TEG under isoflux conditions has never before been studied in detail the influence of leg geometry and energy losses on its performance. Recent investigations [68] show that a variety of factors, including leg lengths, spacing between legs and external load resistances, as well as ambient temperature affect TEG performance. Optimizing all of these aspects experimentally remains a difficulty since the number of trials required to optimize all of the regulating parameters is relatively extensive. The Taguchi approach has been frequently utilized to optimize operational variables because of its unique discipline and the minimal number of tests it necessitates. To improve the surface roughness of a lathe-facing operation [69], diesel-engine system design [70]. Chen et al. [71] and Kishore et al. [72] have utilized Taguchi and ANOVA approaches to optimize the dimensions of heat sinks in the field of TEG. TEG device optimization work has been done using an isothermal heat source condition, which means that the hot side is maintained at a constant temperature, generally less than 500 K, throughout the process. Optimum TEG performance under isoflux heat source conditions has yet to be documented in the literature, hence this is a new finding.

3.4.2. Heat exchanger design characteristics

There are several methods to classify these gadgets depending on their design qualities. Heat exchangers may be classed based on the design of flow configuration, construction method, and heat transfer mechanism. The flow configuration of a heat exchanger, also known as the flow arrangement, refers to the flow direction of the fluids inside the heat exchanger. Heat exchangers utilize four primary flow configurations: co-current flow, countercurrent flow, crossflow, and hybrid flow, as mentioned in Figure 2. Corresponding to the concurrent flow, the fluids flow in the same direction and parallel to one another. This design is less efficient than a counter flow layout; it also provides the best heat exchanger wall thermal homogeneity. Otherwise, the countercurrent flow heat exchangers have their fluids flowing in the opposite direction, creating an antiparallel flow pattern inside the heat exchanger itself.

Meanwhile, fluids flow perpendicularly via crossflow heat exchangers. Equivalent inefficiency to countercurrent and co-current heat exchangers, this flowing design provides a middle ground. In another way, Hybrid flow heat exchangers are a mixture of the flow topologies previously discussed. There are several ways to build a heat exchanger, such as using both counterflow and crossflow arrangements in a single unit. This is the most common form of heat exchanger utilized in applications where space, budget expenses, or temperature and pressure requirements are limiting factors.

Several references in the literature deal with the design of a crossflow heat exchanger, but only a handful are mentioned here. The matrix technique was given by Silaipillayarputhur et al. to construct a crossflow heat exchanger [73]. At each pass of the heat exchanger, the performance of the crossflow heat exchanger was tested. The design engineers could optimize the heat exchanger's performance using this method. Silaipillayarputhur also proposed matrix method validation as an extension. They used matrix approaches to predict the heat exchanger's performance and compared it to the actual data. The creation of performance tables for multi-pass parallel crossflow heat exchangers was studied by Silaipillayarputhur et al. [74]. Incomprehensible tables represented the performance of the heat exchanger at each pass. At each pass, dimensionless metrics such as effectiveness, capacity rate ratio, and the number of transfer units that influence the heat exchanger's steady-state performance were employed to define the heat exchanger's performance.

Much research has been conducted on the transient performance of crossflow heat exchangers. The transient behavior of heat exchangers under dynamic fluid intake temperature fluctuations (hot, cold, or both) has been studied extensively [75,76]. Gartner and Harrison established an experimental setup and conducted a transient experimental analysis of a water-to-air crossflow heat exchanger under periodic temperature fluctuations for experimental measurements [77]. Yuan investigated the impact of several flow maldistribution models on the thermal performance of a three-fluid crossflow heat exchanger [78]. Mishara et al. investigated the nonuniform influence of fluid inlet temperature boundary conditions on the performance of a cross-flow heat exchanger in a transient study [79]. The research specifies and applies two nonuniform temperature boundary conditions to the hot fluid across the input. Their impact is shown and contrasted with a uniform temperature boundary condition. Heat exchanger responses to the combined influence of intake temperature nonuniformity and transient changes are predicted using outlet temperatures. The impact of these nonuniform instances on the transient performance of cross-flow heat exchangers has yet to be thoroughly examined.

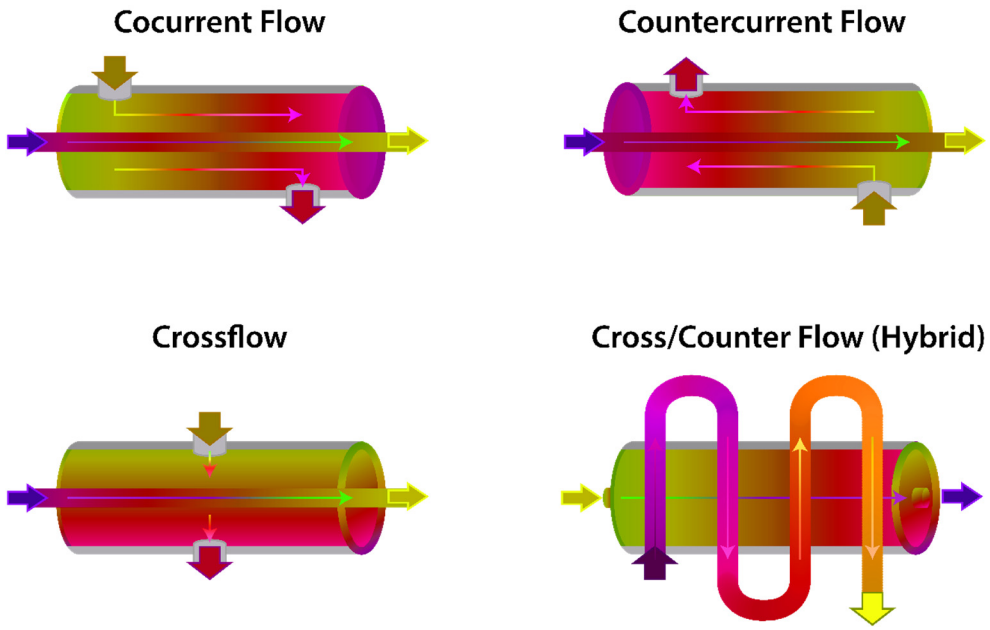

Figure 2. Heat exchanger flow configurations.

While heat exchangers were previously classified according to the flow arrangement utilized, this section categorizes them according to the type of building materials they are made of. To organize these gadgets, we may look at their construction features [80]. As opposed to regenerative heat exchangers, which circulate a single fluid through multiple channels, recuperative heat exchangers circulate a single fluid through multiple channels simultaneously. Regenerative heat exchangers, also known as capacitive heat exchangers or regenerators, enable warm and cold fluids to pass via the same channel [81,82]. In the case of direct and indirect construction characteristics, heat is transferred directly from one fluid to another in direct contact heat exchangers when the fluids are not separated [83]. In contrast, the fluids in indirect heat exchangers stay isolated throughout the heat transfer process by thermally conductive components, such as tubes or plates. Meanwhile, the heat exchanger material and components remain stationary in static regenerators as fluids flow through the device. In contrast, the material and components move throughout the heat transfer process in dynamic regenerators. Both types are at risk of cross-contamination between fluid streams, necessitating careful design considerations during manufacturing.

Heat exchangers use either a single-phase or a two-phase heat transfer mechanism to transport heat. Because there is no phase shift in a single-phase heat exchanger, both the hot and cold fluids stay in their original state of matter throughout heat transfer, resulting in a more efficient transmission of heat [84–86]. Heat is transmitted from one body of water to another by convection, and neither the hotter nor the colder water becomes a gas or solid in the process. During the heat transfer process in two-phase heat exchangers, fluids undergo a phase shift. Consequently, one or both of the fluids involved may undergo a phase shift, which results in a transition from one fluid state to another. There are more design concerns for two-phase heat transfer mechanisms than single-phase heat transfer mechanisms.

3.4.3. Surface profile design of heat exchangers

There are a variety of heat exchangers to choose from, based on the design parameters outlined above. The following are examples of more often used versions in the industry, including heat exchangers with a shell and tubes, heat exchangers with two piping systems, and heat exchangers that use plates. A large number of published works incorporated various characteristics such as corrugation form, plate size, plate distance S, plate number N, and corrugation arrangement as shown in the figures of references [91–108].

Zhang et al. examined the influence of the corrugation profile on the thermal-hydraulic performance of a cross-corrugated plate. Four alternative corrugation profiles were reviewed numerically for the ideal design, including triangular isosceles trapezoidal, rectangular, and elliptic curves [91]. Gulenoglu et al. conducted an experimental examination of three distinct plate geometries' thermal and hydraulic properties [92]. Yang et al. compared a collection of brazed PHEs with various geometrical characteristics. The findings of the experiment indicate that it is the most critical parameter. In general, increasing this angle enhances the single-phase heat transfer. In addition, geometric dimensions influence the heat transmission properties [93].

Durmuş et al. provided an experimental study of three distinct plate heat exchanges (PHEs) of flat PHE, corrugated PHE, and asterisk-type PHE [94]. Comparing the exergy losses of three PHEs revealed that the corrugated PHE was the most effective. The bubble-type [95], horseshoe-type [96–98], and circular spot-type [99] embossing can either improve the thermal-hydraulic performance or the compactness of the heat exchanger, according to prior research. Doo et al. changed the cross-corrugated primary surface by incorporating three unique secondary corrugations [100]. The peak and trough of the sinusoidal plate surface were adjusted using anti-phase, in-phase, and full-wave rectified trough corrugation, respectively, to enhance the performance of PHEs for aero-engine intercooler applications. Lee et al. examined a variety of PHEs with various surface profiles and corrugation furrow shapes [101]. Nilpueng and Wongwises experimented to determine the influence of surface roughness on the heat transfer coefficient and pressure drop of water flow in PHEs [102]. According to the experimental findings, the Nusselt number and friction factors rise as surface roughness increases. Thermal-hydraulic performance is enhanced by surface roughness and decreased by the Reynolds number.

Balaram compared the heat transmission capabilities of rectangular and trapezoidal fin designs. At a specified operating state for unbaffled shell-and-tube heat exchangers (STHX), it can be observed that the heat transfer rate of rectangular fins was superior to that of trapezoidal fins [103]. Parikshite et al. simplified the pressure drop calculations in shell-and-tube heat exchangers [104]. They used the finite element approach in their anticipated model. They demonstrated that the method was extremely successful at forecasting the pressure drop since it needed less time for computation and produced highly accurate predicted results. Chang and Yu suggested an inside spray approach for a shell-and-tube spray evaporator with a triangular pitch. They demonstrated that the heat transfer coefficient on the shell side utilizing the interior spray technique was superior to that of the typical flooded type [105]. Alimoradiand Veysi improved the shell-and-helically-coiled-tube heat exchanger's geometric characteristics. In their investigation, a model that obtained the lowest heat transfer rate per entropy production was deemed the best [106]. Raja et al. included total cost and pressure decrease as additional ideal goals [107]. The objective of their research was to maximize efficiency while reducing overall cost, pressure drop, and entropy production. The multi-objective optimization of Raja's group

is more effective in the actual design of a new heat exchanger than that provided in Ref. [107], although it involves more work. The impact of baffles on the heat transfer and fluid flow properties of the STHXs was also described in [108–114].

3.4.4. Automotive waste heat recovery systems based on TEG

Large multinational automakers such as BMW [115], Ford [116], Renault [117], and Honda [118] have shown an interest in exhaust heat recovery by developing TEG-based systems. The system is rated to output 750 W from several 20 W rated TEGs and uses high temperature TEGs. Multiple tiny parallel passages lined with thermoelectric material are used for the exhaust gases to travel through the Ford system heat exchanger. In this situation, liquid cooling is applied. With 4.6 kg of thermoelectric material, this system is rated to generate a maximum of 400 W. On a diesel truck engine, the Renault system will be employed. It measures 10 × 50 × 31 centimetres. This system employs a liquid-cooled counterflow heat exchanger. A mixture of high-temperature TEGs and low-temperature TEGs was employed at the high-temperature end. At the low-temperature end, a combination of high-temperature TEGs and low-temperature TEG. It is estimated that the simulated system will generate 1 kW. TEGs were positioned on the top and bottom surfaces of the Honda system, which had a basic form of a thin flat rectangular box. The system included 32 x 30 x 30 mm centimeters TEGs and could output up to 500 W.

Goncalves et al., Brito et al., and Martins et al. [119–121] developed a system that uses a heat pipe to remove heat from exhaust gases and a water heat sink to cool the opposite side of the TEGs. Instead of a regular heat pipe, a variable conductance heat pipe is employed in this circumstance. Jang et al. designed a hybrid exhaust heat recovery system incorporating TEGs and heat pipes. Rather than employing typical heat pipes, loop thermosiphons were used in this design [122]. The essential aspect of a TEG's power is the vehicle's speed. The vehicle's speed should be increased to improve TEG performance. More energy is available for conversion into electrical energy as the exhaust temperature rises. When the exhaust temperature rises, dynamic optimization simulations show an increase in ideal length and a decrease in optimal breadth [123]. The temperature has a significant impact on the efficiency and power of a TEG. When the engine is turned between 2500 and 3400 rpm, the temperature of the intake and outflow is shown. The temperature differential between TEG surfaces grows fast as the engine speed increases, increasing output power [124]. It was discovered that if the power generated by the engine is 150 kW, the heat recovery system in the exhaust of the automobile may generate 1.4 kW of electricity and that a waste heat energy recovery system of 500 MW of gas turbine power plant can generate 5.9 MW of electricity [125]. Another experiment was carried out to test the TEG's power output by varying the vehicle's speed.

Based on a dynamic optimization simulation, He et al. discovered that increasing exhaust temperature increased ideal length while decreasing optimal breadth [126]. Furthermore, the thermoelectric characteristics are significant temperature-sensitive, emphasizing the need of a TEG system dynamic operation. The temperature dependency of thermoelectric characteristics substantially influences the power, efficiency, and optimum variables of TEG, according to the simulation findings reported by Meng et al. [127]. Third, the temperature of the TEG's cold end, which is generally connected to the engine coolant, is often affected by the cooling unit's flow rate and radiator functioning. Using a theoretical dynamic model, Gou et al. investigated the dynamic properties of TEG. They discovered that increasing heat dissipation on the cold side might improve TEG performance

more than increasing heat transfer on the hot side [128]. Meng et al. [129] looked at how the TEG modified its behavior when the cold end temperature varied. The output power exhibited response hysteresis to the cold end temperature. In both decreasing and rising occurrences of cold end temperature, TEG conversion efficiency was shown to overshoot and undershoot, respectively. More accurate performance prediction and helpful optimization advice have evolved based on earlier research [127–129] for the transient behavior of TEG. However, a critical feature for a dynamic TEG model that allows for safe TEG system operation and successful after treatment system operation has been overlooked. The most common bismuth tellurium module has a maximum temperature restriction of 250 °C [130], although the exhaust temperatures of a diesel engine and a gasoline engine may reach 400 °C and 800 °C, respectively.

4. Conclusions

TEGs have been demonstrated to have been used in automotive exhaust heat recovery systems, industrial waste heat recovery systems, and perhaps primary power sources. TEGs may be employed as the main power source, as seen in the suggested design. TEGs will become more cost-competitive with conventional petrol generators if the power per unit cost of TEGs continues to rise. TEGs are an excellent method for providing some energy when grid connection is not available, according to the many research and instances mentioned in the paper. This capacity to generate some power also marginally or regularly enhances the efficiency of heat-generating equipment. However, TEGs have limitations, such as relatively low efficiency and maximum surface temperatures.

Furthermore, exhaust gas characteristics and heat exchanger construction are discovered to impact system power production substantially. Because there are so many distinct types of HEXs, deciding on which one to use is quite challenging. Consider the limitations of each heat exchanger type before making a final design choice. The impact of temperature ranges and pressure constraints on thermal performance and pressure drop and the flow capacity of different fluids should be considered in addition to production costs.

Conflict of interest

The authors declare no conflict of interest.

References

1. Amar AB, Kouki AB, Cao H (2015) Power approaches for implantable medical devices. *Sensors (Switzerland)* 15: 28889–28914. https://doi.org/10.3390/s151128889
2. Jaziri N, Boughamoura A, Müller J, et al. (2020) A comprehensive review of thermoelectric generators: Technologies and common applications. *Energy Rep* 6: 264–287. https://doi.org/10.1016/j.egyr.2019.12.011
3. Bombarda P, Invernizzi CM, Pietra C (2010) Heat recovery from diesel engines: A thermodynamic comparison between Kalina and ORC cycles. *Appl Therm Eng* 30: 212–219. https://doi.org/10.1016/j.applthermaleng.2009.08.006
4. Crane D, Jackson G, Holloway D (2001) Towards optimization of automotive waste heat recovery using thermoelectrics. *SAE Tech Pap* 1: 1–13. https://doi.org/10.4271/2001-01-1021

5. Jaziri N, Boughamoura A, Müller J, et al. (2020) A comprehensive review of Thermoelectric generators: Technologies and common applications. *Energy Rep* 6: 264–287. https://doi.org/10.1016/j.egyr.2019.12.011
6. Karvonen M, Kapoor R, Uusitalo A, et al. (2016) Technology competition in the internal combustion engine waste heat recovery: A patent landscape analysis. *J Clean Prod* 112: 3735–3743. https://doi.org/10.1016/j.jclepro.2015.06.031
7. Jia N, Cao J, Tan XY, et al. (2021) Thermoelectric materials and transport physics. *Mater Today Phys* 21: 100519. https://doi.org/10.1016/j.mtphys.2021.100519
8. Knecht W (2008) Diesel engine development in view of reduced emission standards. *Energy* 33: 264–271. https://doi.org/10.1016/j.energy.2007.10.003
9. Saqr KM, Mansour MK, Musa MN (2008) Thermal design of automobile exhaust based Thermoelectric generators: Objectives and challenges. *Int J Automot Technol* 9: 155160. https://doi.org/10.1007/s12239-008-0020-y
10. Zhang X, Chau KT, Chan CC (2008) Overview of Thermoelectric generation for hybrid vehicles. *J Asian Electr Veh* 6: 1119–1124. https://doi.org/10.4130/jaev.6.1119
11. Abedin MJ, Masjuki HH, Kalam MA, et al. (2013) Energy balance of internal combustion engines using alternative fuels. *Renewable Sustainable Energy Rev* 26: 20–33. https://doi.org/10.1016/j.rser.2013.05.049
12. Yüksel F, Ceviz MA (2003) Thermal balance of a four stroke SI engine operating on hydrogen as a supplementary fuel. *Energy* 28: 1069–1080. https://doi.org/10.1016/S0360-5442(03)00090-2
13. Durgun O, Şahin Z (2009) Theoretical investigation of heat balance in direct injection (DI) diesel engines for neat diesel fuel and gasoline fumigation. *Energy Convers Manage* 50: 43–51. https://doi.org/10.1016/j.enconman.2008.09.007
14. Özcan H, Söylemez MS (2006) Thermal balance of a LPG fuelled, four stroke SI engine with water addition. *Energy Convers Manage* 47: 570–581. https://doi.org/10.1016/j.enconman.2005.05.019
15. Mukai K, Iijima T, Miyazaki H, et al. (2005) The effects of design factors of the combustion chamber on heat balance in a gasoline engine. *SAE Tech Pap* 1: 1–9. https://doi.org/10.4271/2005-01-2021
16. Rakopoulos CD, Giakoumis EG (2006) Second-law analyses applied to internal combustion engines operation. *Prog Energy Combust Sci* 32: 2–47. https://doi.org/10.1016/j.pecs.2005.10.001
17. Şahin Z, Durgun O (2007) Theoretical investigation of effects of light fuel fumigation on diesel engine performance and emissions. *Energy Convers Manage* 48: 1952–1964. https://doi.org/10.1016/j.enconman.2007.01.027
18. Ramadhas AS, Jayaraj S, Muraleedharan C (2006) Theoretical modeling and experimental studies on biodiesel-fueled engine. *Renewable Energy* 31: 1813–1826. https://doi.org/10.1016/j.renene.2005.09.011
19. Liu Y, Reitz RD (1998) Modeling of heat conduction within chamber walls for multidimensional internal combustion engine simulations. *Int J Heat Mass Transf* 41: 859–869.
20. Lounici MS, Loubar K, Balistrou M, et al. (2011) Investigation on heat transfer evaluation for a more efficient two-zone combustion model in the case of natural gas SI engines. *Appl Therm Eng* 31: 319–328. https://doi.org/10.1016/j.applthermaleng.2010.09.012

21. Dado B, Gelbstein Y, Dariel MP (2010) Nucleation of nanosize particles following the spinodal decomposition in the pseudo-ternary Ge0.6Sn0.1Pb0.3Te compound. *Scr Mater* 62: 89–92. https://doi.org/10.1016/j.scriptamat.2009.09.029
22. Komisarchik G, Gelbstein Y, Fuks D (2017) Solubility of Ti in thermoelectric PbTe compound. *Intermetallics* 89: 16–21. https://doi.org/10.1016/j.intermet.2017.05.016
23. Meroz O, Gelbstein Y (2018) Thermoelectric Bi_2Te_3-xSex alloys for efficient thermal to electrical energy conversion. *Phys Chem Chem Phys* 20: 4092–4099.
24. Sadia Y, Elegrably M, Ben-Nun O, et al. (2013) Submicron features in higher manganese silicide. *J Nanomater* 2013: 5–10. https://doi.org/10.1155/2013/701268
25. Zilber T, Cohen S, Fuks D, et al. (2019) TiNiSn half-Heusler crystals grown from metallic flux for thermoelectric applications. *J Alloys Comp* 781: 1132–1138. https://doi.org/10.1016/j.jallcom.2018.12.165
26. Suwardi A, Cao J, Hu L, et al. (2020) Tailoring the phase transition temperature to achieve high-performance cubic GeTe-based thermoelectrics. *J Mater Chem A* 8: 18880–18890. https://doi.org/10.1039/D0TA06013E
27. Suwardi A, Cao J, Zhao Y, et al. (2020) Achieving high thermoelectric quality factor toward high figure of merit in GeTe. *Mater Today Phys* 14: 100239. https://doi.org/10.1016/j.mtphys.2020.100239
28. Chen X, Dai W, Wu T, et al. (2018) Thin film thermoelectric materials: Classification, characterization, and potential for wearable applications. *Coatings* 8: 1–16. https://doi.org/10.3390/coatings8070244
29. Ren P, Liu Y, He J, et al. (2018) Recent advances in inorganic material thermoelectrics. *Inorg Chem Front* 5: 2380–2398. https://doi.org/10.1039/C8QI00366A
30. Wong-Ng W, Yan Y, Otani M, et al. (2015) High throughput screening tools for thermoelectric materials. *J Electron Mater* 44: 1688–1696. https://doi.org/10.1007/s11664-014-3519-1
31. Bhattacharya S, Madsen GKH (2015) High-throughput exploration of alloying as design strategy for thermoelectrics. *Phys Rev B: Condens Matter Mater Phys* 92: 1–9. https://doi.org/10.48550/arXiv.1508.03477
32. Gibbs ZM, Ricci F, Li G, et al. (2017) Effective mass and Fermi surface complexity factor from ab initio band structure calculations. *Npj Comput Mater* 3: 1–6. https://doi.org/10.1038/s41524-017-0013-3
33. Liu R, Chen H, Zhao K, et al. (2017) Entropy as a gene-like performance indicator promoting thermoelectric materials. *Adv Mater* 29: 1–7. https://doi.org/10.1002/adma.201702712
34. Fan Z, Wang H, Wu Y, et al. (2017) Thermoelectric performance of PbSnTeSe high-entropy alloys. *Mater Res Lett* 5: 187–194. https://doi.org/10.1080/21663831.2016.1244116
35. Fan Z, Wang H, Wu Y, et al. (2016) Thermoelectric high-entropy alloys with low lattice thermal conductivity. *RSC Adv* 6: 52164–52170. https://doi.org/10.1039/C5RA28088E
36. Zhu Q, Wang S, Wang X, et al. (2021) Bottom-up engineering strategies for high-performance thermoelectric materials. *Nano-Micro Letters* 13: 1–38. Available from: https://link.springer.com/article/10.1007/s40820-021-00637-z.
37. Kinsella CE, O'Shaughnessy SM, Deasy MJ, et al. (2014) Battery charging considerations in small scale electricity generation from a thermoelectric module. *Appl Energy* 114: 80–90. https://doi.org/10.1016/j.apenergy.2013.09.025

38. Kawajiri K, Kishita Y, Shinohara Y (2021) Life cycle assessment of thermoelectric generators (TEGs) in an automobile application. *Sustainability* 13: 1–13. https://doi.org/10.3390/su132413630
39. Karri MA, Thacher EF, Helenbrook BT (2011) Exhaust energy conversion by thermoelectric generator: Two case studies. *Energy Convers Manage* 52: 1596–1611. https://doi.org/10.1016/j.enconman.2010.10.013
40. Liu X, Deng YD, Li Z, et al. (2015) Performance analysis of a waste heat recovery thermoelectric generation system for automotive application. *Energy Convers Manage* 90: 121–127. https://doi.org/10.1016/j.enconman.2014.11.015
41. Wang Y, Dai C, Wang S (2013) Theoretical analysis of a thermoelectric generator using exhaust gas of vehicles as heat source. *Appl Energy* 112: 1171–1180. https://doi.org/10.1016/j.apenergy.2013.01.018
42. Liu X, Li C, Deng YD, et al. (2015) An energy-harvesting system using thermoelectric power generation for automotive application. *Int J Electr Power Energy Syst* 67: 510–516. https://doi.org/10.1016/j.ijepes.2014.12.045
43. Wang P, Ji C, Tang B, et al. (2010) Effect of common rail system on vehicle engine combustion performance. *Proc-2010 Int Conf Optoelectron Image Process ICOIP 2010* 1: 464–467. https://doi.org/10.1109/CCIENG.2011.6007975
44. Huang K, Chang H, Qin J, et al. (2011) The exploration of HCCI combustion in the high-power direct-injection diesel engine. *CCIE 2011-Proc 2011 IEEE 2nd Int Conf Comput Control Ind Eng* 1: 133–135. https://doi.org/10.1109/CCIENG.2011.6007975
45. Arsie I, Cricchio A, Pianese C, et al. (2014) A comprehensive powertrain model to evaluate the benefits of electric turbo compound (ETC) in reducing CO_2 emissions from small diesel passenger cars. *SAE Tech Pap 1*. https://doi.org/10.4271/2014-01-1650
46. Hatami M, Ganji DD, Gorji-Bandpy M (2014) A review of different heat exchangers designs for increasing the diesel exhaust waste heat recovery. *Renewable Sustainable Energy Rev* 37: 168–181. https://doi.org/10.1016/j.rser.2014.05.004
47. Thomas J (2014) Drive cycle powertrain efficiencies and trends derived from EPA vehicle dynamometer results. *SAE Int J Passeng Cars-Mech Syst* 7: 1374–1384. https://doi.org/10.4271/2014-01-2562
48. Liming F, Wenzhi G, Hao Q, et al. (2010) Heat recovery from internal combustion engine with Rankine cycle. *Asia-Pacific Power Energy Eng Conf APPEEC* 1: 2–5. https://doi.org/10.1109/APPEEC.2010.5448861
49. Mingshan W, Jinli F, Chaochen M, et al. (2011) Waste heat recovery from heavy-duty diesel engine exhaust gases by medium temperature ORC system. *Sci China Technol Sci* 54: 2746–2753. https://doi.org/10.1007/s11431-011-4547-1
50. Amicabile S, Lee JI, Kum D (2015) A comprehensive design methodology of organic Rankine cycles for the waste heat recovery of automotive heavy-duty diesel engines. *Appl Therm Eng* 87: 574–585. https://doi.org/10.1016/j.applthermaleng.2015.04.034
51. Kobayashi H, Yaji K, Yamasaki S, et al. (2021) Topology design of two-fluid heat exchange. *Struct Multidiscip Optim* 63: 821–834. https://doi.org/10.48550/arXiv.2005.08870
52. Li J, Zhou L, Pan K, et al. (1995) Evaluation of the thermodynamic process of indirect injection diesel engines by the first and second law. *SAE Tech Pap*: 09: 1–13. https://doi.org/10.4271/952055

53. Ghazikhani M, Feyz ME, Joharchi A (2010) Experimental investigation of the exhaust gas recirculation effects on irreversibility and brake specific fuel consumption of indirect injection diesel engines. *Appl Therm Eng* 30: 1711–1718. https://doi.org/10.1016/j.applthermaleng.2010.03.030
54. Ozcan H (2010) Hydrogen enrichment effects on the second law analysis of a lean burn natural gas engine. *Int J Hydrogen Energy* 35: 1443–1452. https://doi.org/10.1016/j.ijhydene.2009.11.039
55. Rakopoulos CD, Kyritsis DC (2001) Comparative second-law analysis of internal combustion enginge operation for methane, methanol, and dodecane fuels. *Energy* 26: 705–722. https://doi.org/10.1016/S0360-5442(01)00027-5
56. Saidur R, Rezaei M, Muzammil WK, et al. (2012) Technologies to recover exhaust heat from internal combustion engines. *Renewable Sustainable Energy Rev* 16: 5649–5659. https://doi.org/10.1016/j.rser.2012.05.018
57. Duparchy A, Leduc P, Bourhis G, et al. (2009) Heat recovery for next generation of hybrid vehicles: Simulation and design of a Rankine cycle system. *24th Int Batter Hybrid Fuel Cell Electr Veh Symp Exhib 2009, EVS* 24. 2: 1408–1424. https://doi.org/10.3390/wevj3030440
58. Conklin JC, Szybist JP (2010) A highly efficient six-stroke internal combustion engine cycle with water injection for in-cylinder exhaust heat recovery. *Energy* 35: 1658–1664. https://doi.org/10.1016/j.energy.2009.12.012
59. Hosseini MJ, Ranjbar AA, Sedighi K, et al. (2012) A combined experimental and computational study on the melting behavior of a medium temperature phase change storage material inside shell and tube heat exchanger. *Int Commun Heat Mass Transf* 39: 1416–1424. https://doi.org/10.1016/j.icheatmasstransfer.2012.07.028
60. Jamshidi N, Farhadi M, Ganji DD, et al. (2013) Experimental analysis of heat transfer enhancement in shell and helical tube heat exchangers. *Appl Therm Eng* 51: 644–652. https://doi.org/10.1016/j.applthermaleng.2012.10.008
61. Xu HJ, Xing ZB, Wang FQ, et al. (2019) Review on heat conduction, heat convection, thermal radiation and phase change heat transfer of nanofluids in porous media: Fundamentals and applications. *Chem Eng Sci* 195: 462–483. https://doi.org/10.1016/j.ces.2018.09.045
62. Xu HJ, Gong L, Zhao CY, et al. (2015) Analytical considerations of local thermal non-equilibrium conditions for thermal transport in metal foams. *Int J Therm Sci* 95: 73–87. https://doi.org/10.1016/j.ijthermalsci.2015.04.007
63. Boomsma K, Poulikakos D (2011) Erratum: On the effective thermal conductivity of a three-dimensionally structured fluid-saturated metal foam. *Int J Heat Mass Transf* 54: 746–748. https://doi.org/10.1016/S0017-9310(00)00123-X
64. Brinkman HC (1952) The viscosity of concentrated suspensions and solutions. *J Chem Phys* 20: 571. https://doi.org/10.1063/1.1700493
65. Buongiorno J (2006) Convective transport in nanofluids. *J Heat Transfer* 128: 240–250. https://doi.org/10.1115/1.2150834
66. Calmidi VV, Mahajan RL (1999) The effective thermal conductivity of high porosity fibrous metal foams. *J Heat Transfer* 121: 466–471. https://doi.org/10.1115/1.2826001
67. Das SK, Putra N, Thiesen P, et al. (2003) Temperature dependence of thermal conductivity enhancement for nanofluids. *J Heat Transfer* 125: 567–574. https://doi.org/10.1115/1.1571080

68. Gao L, Zhou XF (2006) Differential effective medium theory for thermal conductivity in nanofluids. *Phys Lett Sect A Gen At Solid State Phys* 348: 355–360. https://doi.org/10.1016/j.physleta.2005.08.069
69. Manohara R, Harinath MA (2019) Application of Taguchi method for optimization of process parameters in drilling operation. *Int J Trend Sci Res Dev* 3: 1052–1057. https://doi.org/10.31142/ijtsrd24003
70. Alkidas AC, Battiston PA, Kapparos DJ (2004) Thermal studies in the exhaust system of a diesel-powered light-duty vehicle. *SAE Tech Pap* 1: 1–21. https://doi.org/10.4271/2004-01-0050
71. Kishore RA, Kumar P, Priya S (2018) A comprehensive optimization study on Bi_2Te_3 -based thermoelectric generators using the Taguchi method. *Sustainable Energy Fuels* 2: 175–190. https://doi.org/10.1039/C7SE00437K
72. Kang CC, Yamauchi KA, Vlassakis J, et al. (2016) Single cell-resolution western blotting. *Nat Protoc* 11: 1508–1530. https://doi.org/10.1038/nprot.2016.089
73. Silaipillayarputhur K, Idem S (2013) A general matrix approach to model steady-state performance of crossflow heat exchangers. *Heat Transf Eng* 34: 338–348. https://doi.org/10.1080/01457632.2013.716347
74. Silaipillayarputhur K, Al Mughanam T (2018) Performance charts for multi-pass parallel crossflow heat exchangers. *Int J Mech Eng Robot Res* 7: 478–482. https://doi.org/10.18178/ijmerr.7.5.478-482
75. Romie FE (1983) Transient response of gas-to-gas crossflow heat exchangers with neither gas mixed. *J Heat Transfer* 105: 563–570. https://doi.org/10.1016/0017-9310(91)90249-E
76. Gao T, Geer J, Sammakia B (2014) Nonuniform temperature boundary condition effects on data center cross flow heat exchanger dynamic performance. *Int J Heat Mass Transf* 79: 1048–1058. https://doi.org/10.1016/j.ijheatmasstransfer.2014.09.011
77. Gao T, Sammakia BG, Geer FJ, et al. (2014) Dynamic analysis of cross flow heat exchangers in data centers using transient effectiveness method. *IEEE Trans Components, Packag Manuf Technol* 4: 1925–1935. https://doi.org/10.1109/TCPMT.2014.2369256
78. Yuan P (2003) Effect of inlet flow maldistribution on the thermal performance of a three-fluid crossflow heat exchanger. *Int J Heat Mass Transf* 46: 3777–3787. https://doi.org/10.1016/S0017-9310(03)00196-0
79. Mishra M, Das PK, Sarangi S (2008) Effect of temperature and flow nonuniformity on transient behaviour of crossflow heat exchanger. *Int J Heat Mass Transf* 51: 2583–2592. https://doi.org/10.1016/j.ijheatmasstransfer.2007.07.054
80. Guo D, Gao J, Yu YJ, et al. (2014) Design and modeling of a fluid-based micro-scale electrocaloric refrigeration system. *Int J Heat Mass Transf* 72: 559–564. https://doi.org/10.1016/j.ijheatmasstransfer.2014.01.043
81. Jia Y, Sungtaek Ju Y (2012) A solid-state refrigerator based on the electrocaloric effect. *Appl Phys Lett* 100. https://doi.org/10.1063/1.4729038
82. Ossmer H, Wendler F, Gueltig M, et al. (2016) Energy-efficient miniature-scale heat pumping based on shape memory alloys. *Smart Mater Struct* 25: 1–13. Avaiable from: https://iopscience.iop.org/article/10.1088/0964-1726/25/8/085037.
83. Park SIl (1996) Performance analysis of a moving-bed heat exchanger in vertical pipes. *Energy* 21: 911–918. https://doi.org/10.1016/0360-5442(96)00027-8

84. Rahimi A, Niksiar A (2013) A general model for moving-bed reactors with multiple chemical reactions part I: Model formulation. *Int J Miner Process* 124: 58–66. https://doi.org/10.1016/j.minpro.2013.02.015
85. García-Triñanes P, Seville JPK, Ansart R, et al. (2018) Particle motion and heat transfer in an upward-flowing dense particle suspension: Application in solar receivers. *Chem Eng Sci* 177: 313–322. https://doi.org/10.1016/j.ces.2017.11.041
86. Yusuf R, Melaaen MC, Mathiesen V (2005) Convective heat and mass transfer modeling in gas-fluidized beds. *Chem Eng Technol* 28: 13–24. https://doi.org/10.1002/ceat.200407014
87. Zhang Y, Jiang C, Yang Z, et al. (2016) Numerical study on heat transfer enhancement in capsule-type plate heat exchangers. *Appl Therm Eng* 108: 1237–1242. https://doi.org/10.1016/j.applthermaleng.2016.08.033
88. Song JW, Wang F, Cheng L (2012) Experimental study and analysis of a novel multi-media plate heat exchanger. *Sci China Technol Sci* 55: 2157–2162. https://doi.org/10.1007/s11431-012-4931-5
89. Villanueva HHS, de Mello PEB (2015) Heat transfer and pressure drop correlations for finned plate ceramic heat exchangers. *Energy* 88: 118–125. https://doi.org/10.1016/j.energy.2015.04.017
90. Kim M, Baik YJ, Park SR, et al. (2010) Experimental study on corrugated crossflow air-cooled plate heat exchangers. *Exp Therm Fluid Sci* 34: 1265–1272. https://doi.org/10.1016/j.expthermflusci.2010.05.007
91. Zhang L, Che D (2011) Influence of corrugation profile on the thermalhydraulic performance of cross-corrugated plates. *Numer Heat Transf Part A Appl* 59: 267–296. https://doi.org/10.1080/10407782.2011.540963
92. Gulenoglu C, Akturk F, Aradag S, et al. (2014) Experimental comparison of performances of three different plates for gasketed plate heat exchangers. *Int J Therm Sci* 75: 249–256. https://doi.org/10.1016/j.ijthermalsci.2013.06.012
93. Yang J, Jacobi A, Liu W (2017) Heat transfer correlations for single-phase flow in plate heat exchangers based on experimental data. *Appl Therm Eng* 113: 1547–1557. https://doi.org/10.1016/j.applthermaleng.2016.10.147
94. Durmuş A, Benli H, Kurtbaş I, et al. (2009) Investigation of heat transfer and pressure drop in plate heat exchangers having different surface profiles. *Int J Heat Mass Transf* 52: 1451–1457. https://doi.org/10.1016/j.ijheatmasstransfer.2008.07.052
95. Seo JW, Kim YH, Kim D, et al. (2015) Heat transfer and pressure drop characteristics in straight microchannel of printed circuit heat exchangers. *Entropy* 17: 3438–3457. https://doi.org/10.3390/e17053438
96. Gao T, Sammakia BG, Geer J, et al. (2014) Dynamic analysis of cross flow heat exchangers in data centers using transient effectiveness Method. *IEEE Trans Components, Packag Manuf Technol* 4: 1925–1935. Avaiable from: https://ieeexplore.ieee.org/document/6963402.
97. Vintrou S, Bougeard D, Russeil S, et al. (2013) Quantitative infrared investigation of local heat transfer in a circular finned tube heat exchanger assembly. *Int J Heat Fluid Flow* 44: 197–207. https://doi.org/10.1016/j.ijheatfluidflow.2013.05.019
98. Monteiro DB, de Mello PEB (2012) Thermal performance and pressure drop in a ceramic heat exchanger evaluated using CFD simulations. *Energy* 45: 489–496. https://doi.org/10.1016/j.energy.2012.02.012

99. Zhang C, Wang D, Han Y, et al. (2017) Experimental and numerical investigation on the exergy and entransy performance of a novel plate heat exchanger. *Exp Heat Transf* 30: 162–177. https://doi.org/10.1080/08916152.2016.1179358
100. Doo JH, Ha MY, Min JK, et al. (2012) An investigation of cross-corrugated heat exchanger primary surfaces for advanced intercooled-cycle aero engines (Part-I: Novel geometry of primary surface). *Int J Heat Mass Transf* 55: 5256–5267. https://doi.org/10.1016/j.ijheatmasstransfer.2013.01.084
101. Lee JM, Kwan PW, Son CM, et al. (2015) Characterizations of aerothermal performance of novel cross-corrugated plate heat exchangers for advanced cycle aero-engines. *Int J Heat Mass Transf* 85: 166–180. https://doi.org/10.1016/j.ijheatmasstransfer.2013.01.084
102. Nilpueng K, Wongwises S (2015) Experimental study of single-phase heat transfer and pressure drop inside a plate heat exchanger with a rough surface. *Exp Therm Fluid Sci* 68: 268–275. https://doi.org/10.1016/j.expthermflusci.2015.04.009
103. Kundu B (2015) Beneficial design of unbaffled shell-and-tube heat exchangers for attachment of longitudinal fins with trapezoidal profile. *Case Stud Therm Eng* 5: 104–112. https://doi.org/10.1016/j.csite.2015.03.001
104. Parikshit B, Spandana KR, Krishna V, et al. (2015) A simple method to calculate shell side fluid pressure drop in a shell and tube heat exchanger. *Int J Heat Mass Transf* 84: 700–712. https://doi.org/10.1016/j.ijheatmasstransfer.2015.01.068
105. Chang TB, Yu LY (2015) Optimal nozzle spray cone angle for triangular-pitch shell-and-tube interior spray evaporator. *Int J Heat Mass Transf* 85: 463–472. https://doi.org/10.1016/j.ijheatmasstransfer.2015.01.123
106. Alimoradi A, Veysi F (2017) Optimal and critical values of geometrical parameters of shell and helically coiled tube heat exchangers. *Case Stud Therm Eng* 10: 73–78. https://doi.org/10.1016/j.csite.2017.03.003
107. Raja BD, Jhala RL, Patel V (2017) Many-objective optimization of shell and tube heat exchanger. *Therm Sci Eng Prog* 2: 87–101. https://doi.org/10.1016/j.tsep.2017.05.003
108. Gao B, Bi Q, Nie Z, et al. (2015) Experimental study of effects of baffle helix angle on shell-side performance of shell-and-tube heat exchangers with discontinuous helical baffles. *Exp Therm Fluid Sci* 68: 48–57. https://doi.org/10.1016/j.expthermflusci.2015.04.011
109. Salahuddin U, Bilal M, Ejaz H (2015) A review of the advancements made in helical baffles used in shell and tube heat exchangers. *Int Commun Heat Mass Transf* 67: 104–108. https://doi.org/10.1016/j.icheatmasstransfer.2015.07.005
110. Yang JF, Zeng M, Wang QW (2015) Numerical investigation on combined single shell-pass shell-and-tube heat exchanger with two-layer continuous helical baffles. *Int J Heat Mass Transf* 84: 103–113. https://doi.org/10.1016/j.ijheatmasstransfer.2014.12.042
111. Zhou GY, Xiao J, Zhu L, et al. (2015) A Numerical Study on the Shell-Side Turbulent Heat Transfer Enhancement of Shell-and-Tube Heat Exchanger with Trefoil-Hole Baffles. *Energy Procedia* 75: 3174–3179. https://doi.org/10.1016/j.egypro.2015.07.656
112. Wen J, Yang H, Jian G, et al. (2016) Energy and cost optimization of shell and tube heat exchanger with helical baffles using Kriging metamodel based on MOGA. *Int J Heat Mass Transf* 98: 29–39. https://doi.org/10.1016/j.ijheatmasstransfer.2016.02.084

113. Du BC, He YL, Wang K, et al. (2017) Convective heat transfer of molten salt in the shell-and-tube heat exchanger with segmental baffles. *Int J Heat Mass Transf* 113: 456–465. https://doi.org/10.1016/j.ijheatmasstransfer.2017.05.075
114. Wen J, Yang H, Wang S, et al. (2017) PIV experimental investigation on shell-side flow patterns of shell and tube heat exchanger with different helical baffles. *Int J Heat Mass Transf* 104: 247–259. https://doi.org/10.1016/j.ijheatmasstransfer.2016.08.048
115. Crane D, Lagrandeur J, Jovovic V, et al. (2013) TEG on-vehicle performance and model validation and what it means for further teg development. *J Electron Mater* 42: 1582–1591. https://doi.org/10.1007/s11664-012-2327-8
116. Mori M, Yamagami T, Sorazawa M, et al. (2011) Simulation of fuel economy effectiveness of exhaust heat recovery system using thermoelectric generator in a series hybrid. *SAE Int J Mater Manuf* 4: 1268–1276. https://doi.org/10.4271/2011-01-1335
117. Hussain QE, Brigham DR, Maranville CW (2009) Thermoelectric exhaust heat recovery for hybrid vehicles. *SAE Tech Pap* 2: 1132–1142. https://doi.org/10.4271/2009-01-1327
118. Espinosa N, Lazard M, Aixala L, et al. (2010) Modeling a thermoelectric generator applied to diesel automotive heat recovery. *J Electron Mater* 39: 1446–1455. https://doi.org/10.1007/s11664-010-1305-2
119. Gonçalves VM, Maia CA, Hardouin L (2012) On the solution of Max-plus linear equations with application on the control of TEGs. *IFAC Proc* 45: 91–97. https://doi.org/10.3182/20121003-3-MX-4033.00018
120. Brito FP, Goncalves LM, Martins J, et al. (2013) Influence of heat pipe operating temperature on exhaust heat thermoelectric generation. *SAE Int J Passeng Cars-Mech Syst* 6: 652–664. https://doi.org/10.4271/2013-01-0559
121. Martins J, Goncalves LM, Antunes J, et al. (2011) Thermoelectric exhaust energy recovery with temperature control through heat pipes. *SAE 2011 World Congr Exhib* 1: 1–16. Avaiable from: https://core.ac.uk/download/pdf/55616825.pdf.
122. Jang JC, Chi RG, Rhi SH, et al. (2015) Heat pipe-assisted thermoelectric power generation technology for waste heat recovery. *J Electron Mater* 44: 2039–2047. https://doi.org/10.1007/s11664-015-3653-4
123. Lan S, Yang Z, Chen R, et al. (2018) A dynamic model for thermoelectric generator applied to vehicle waste heat recovery. *Appl Energy* 210: 327–338. https://doi.org/10.1016/j.apenergy.2017.11.004
124. Tang ZB, Deng YD, Su CQ, et al. (2015) A research on thermoelectric generator's electrical performance under temperature mismatch conditions for automotive waste heat recovery system. *Case Stud Therm Eng* 5: 143–150. https://doi.org/10.1016/j.csite.2015.03.006
125. Orr B, Akbarzadeh A (2017) Prospects of waste heat recovery and power generation using thermoelectric generators. *Energy Procedia* 110: 250–255. https://doi.org/10.1016/j.egypro.2017.03.135
126. He W, Wang S, Yue L (2017) High net power output analysis with changes in exhaust temperature in a thermoelectric generator system. *Appl Energy* 196: 259–267. https://doi.org/10.1016/j.apenergy.2016.12.078

127. Fankai M, Lingen Ch, Sun FR (2012) Effects of temperature dependence of thermoelectric properties on the power and efficiency of a multielement thermoelectric generator. *Int J Energy Environ Eng* 3: 137–150. Available from: https://www.ijee.ieefoundation.org/vol3/issue1/IJEE_14_v3n1.pdf.
128. Gou X, Yang S, Xiao H, et al. (2013) A dynamic model for thermoelectric generator applied in waste heat recovery. *Energy* 52: 201–209. https://doi.org/10.1016/j.apenergy.2017.11.004
129. Meng JH, Zhang XX, Wang XD (2014) Dynamic response characteristics of thermoelectric generator predicted by a three-dimensional heat-electricity coupled model. *J Power Sources* 245: 262–269. https://doi.org/10.1016/j.jpowsour.2013.06.127
130. Hsu CT, Huang GY, Chu HS, et al. (2011) An effective Seebeck coefficient obtained by experimental results of a thermoelectric generator module. *Appl Energy* 88: 5173–5179. https://doi.org/10.1016/j.apenergy.2011.07.033

AIMS Press